Technical Paper

ISSN 1997-1400 Int. J. Pavement Res. Technol. 3(6):343-351

Influence of Aging on Surface Free Energy of Asphalt Binder

Jianming Wei[1+] and Yuzhen Zhang[2]

Abstract: Surface free energy of asphalt binder is related to the work of cohesion within the binder and the work of adhesion between binder and aggregate. The sessile drop method was used in this study to measure the contact angle between asphalt binders and three probe liquids. From these measurements, the surface free energies of the asphalt binder were determined using the Owens-Wendt method. The rolling thin film oven test (RTFOT) and pressure aging vessel (PAV) test were carried out to age asphalt binders, through which the influence of aging on the surface free energy was investigated. Results indicated that both RTFOT and PAV aging processes can reduce the surface free energy for most asphalt binders, which means the asphalt binder has the tendency to crack due to RTFOT and PAV aging.

Key words*: Asphalt binder; Contact angle; PAV-aging; RTFOT-aging; Surface free energy.*

Introduction

The performance of asphalt binder closely relates to its durability, and oxidative aging is one of the main factors. Aging can cause hardening of asphalt binder, and consequently, may make a contribution to the deterioration of asphalt pavements [1]. The aging process can be divided into two phases, which are short-term aging and long-term aging, respectively. During the asphalt mixture construction the short-term aging happens, which is primarily associated with the loss of volatile components and oxidation of the binder. Long-term aging is controlled by progressive oxidation, which happens in the field [2].

Surface free energy of asphalt binder can be used to characterize the work of cohesion, and also can be used to evaluate the work of adhesion with the combination of the surface free energy of aggregate in the presence of water, which is related to the moisture damage of asphalt pavement [3]. Masad et al. [4] had already used work of cohesion of the asphalt binder to predict the fatigue cracking characteristics of asphalt mastics and mixtures. In a recent study by Wasiuddin et al. [5], it was found the surface free energies of two aggregates were reduced after styrene-butadiene rubber (SBR) treatment. And the free energy of adhesion between binder and aggregate was increased by SBR coating. Gandhi et al. [6] and Hossain et al. [7] evaluated the influence of anti-stripping agents on performances the binders and mixtures in terms of moisture damage.

Most previous studies have focused on surface free energy of neat asphalt binder. However, few researches have considered the influence of aging on surface free energy. Cheng et al. [8] found that aging reduced the surface free energy of asphalt binder significantly after studying the high cure rubber (HCR) asphalt binders, which were aged in the laboratory for 3 and 6 months. Wasiuddin et al. [9] pointed out that the surface free energy was decreased if the binder was added of anti-strip additives. Howson et al. [10] used stirred air flow test and pressure aging vessel test to simulate short-term aging and long-term aging processes, respectively. And it was found that surface energies of most binders were reduced after aging. Some cases had fluctuated results.

The objective of the study reported in this paper was to investigate the influence of aging on the surface free energy of asphalt binder. Asphalt samples were aged by rolling thin film oven test (RTFOT), and followed by pressure aging vessel (PAV) test. Sessile drop method was employed to determine the surface free energy of each asphalt binder.

Experimental Work

Asphalt Binders

Five different strategic highway research program (SHRP) core asphalt binders were chosen in this study, which were from different crude sources or had different grades and different chemical compositions. These binders were coded with three capital letters followed by an Arabic numeral. Table 1 shows the crude source, performance grade, and component analysis, as well as the wax content of the asphalt binders [11].

Aging Procedures

Aging of the asphalt samples was carried out with RTFOT and PAV followed. The RTFOT aging was conducted at 163°C for 45, 85, 135, and 175*mins*, respectively. Except aging time, the rest conditions were complied with AASHTO T 240. The PAV aging was performed for 20*hrs* at 100°C and with an air pressure of 2.1*MPa*, according to AASHTO R 28.

The RTFOT aged binders were coded as "Original binder code-R-aging time", and PAV aged binders were coded as "Original

[1] Research Engineer, PhD, State Key Laboratory of Heavy Oil Processing, Heavy Oil Research Institute, China University of Petroleum, China.
[2] Professor, PhD, State Key Laboratory of Heavy Oil Processing, Heavy Oil Research Institute, China University of Petroleum, China.
[+] Corresponding Author: E-mail jianming_wei@yahoo.com
Note: Submitted January 9, 2010; Revised April 21, 2010; Accepted May 27, 2010.

Table 1. Physical and Chemical Properties of the SHRP Asphalt Binders in this Study [11].

Asphalt Binder	Crude Source	PG	wt%				Wax/ %
			Saturates	Napthene Aromatics	Polar Aromatics	Asphaltenes (*n*-Heptane)	
AAD-1	California Coastal	58-28	8.6	25.1	41.3	20.5	1.94
AAG-2	California Valley	58-16	6.6	35.3	51.0	5.0	1.11
AAK-1	Boscan	64-22	5.1	30.0	41.8	20.1	1.17
AAM-1	West Texas Intermed.	64-16	1.9	41.9	50.3	4.0	4.21
ABM-1	California Valley	58-10	9.0	29.6	52.4	7.1	1.10

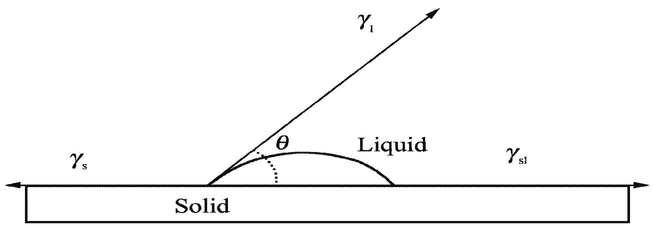

Fig. 1. Contact Angle for a Liquid Drop on the Solid Surface.

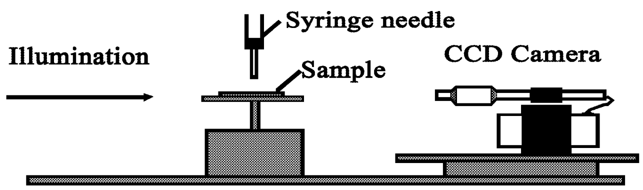

Fig. 2. Sketch Map of Static Contact Angle Measurement Device.

binder code-R-aging time/PAV". The AAD-1 binder was taken as an example to illustrate this. After 45*mins* of RTFOT aging, the sample was named as "AAD-1-R-45". And after PAV aging for "AAD-1-R-45", the aged sample was named as "AAD-1-R-45/PAV".

Determination of Surface Free Energy and Contact Angle Measurement

Determination of Surface Free Energy

Contact angle measurement was used to determine the surface free energy of asphalt binder in this study. When one drop of a liquid is placed on the surface of a solid, the contact angle (θ) depends on three energies, which are the surface free energy of the solid (γ_s), the surface free energy of the liquid (γ_l), and the interfacial free energy of the liquid and solid (γ_{sl}), as illustrated in Fig. 1. At equilibrium, Young's equation [12] can describe the interfacial free energy:

$$\gamma_s = \gamma_{sl} + \gamma_l \cos\theta \tag{1}$$

According to Fowkes [13], the surface free energy of a liquid γ_l and a solid γ_s can be expressed as the sum of two components:

$$\gamma_l = \gamma_l^d + \gamma_l^p;\quad \gamma_s = \gamma_s^d + \gamma_s^p \tag{2}$$

Where γ_l^d and γ_l^p are the dispersion (Lifshitz-van der Waals force) and polar (acid-base force) components of the surface free energy of the liquid; γ_s^d and γ_s^p are the dispersion and polar components of the surface free energy of the solid.

Owen and Wendt [14] developed Fowkes' theory and established the following equation:

$$\gamma_{sl} = \gamma_s + \gamma_l - 2\sqrt{\gamma_s^d \gamma_l^d} - 2\sqrt{\gamma_s^p \gamma_l^p} \tag{3}$$

By combining the Eqs. (1), (2), and (3), the following expression can be obtained:

$$\frac{(1+\cos\theta)}{2}\frac{\gamma_l}{\sqrt{\gamma_l^d}} = \sqrt{\gamma_s^p} \times \sqrt{\frac{\gamma_l^p}{\gamma_l^d}} + \sqrt{\gamma_s^d} \tag{4}$$

The component of surface free energy can be determined through this procedure: plotting $\frac{(1+\cos\theta)}{2}\frac{\gamma_l}{\sqrt{\gamma_l^d}}$ against $\sqrt{\frac{\gamma_l^p}{\gamma_l^d}}$ for different test liquids, the square of the slope and the intercept are the polar component γ_s^p, and the dispersion component γ_s^d of the solid surface free energy, respectively.

Contact Angle Measurement

Contact angles on the asphalt surface were measured using sessile drop method with a Drop Shape Analysis System 10 [15], which is composed of an illumination device, a charge-coupled device (CCD) camera, three micro syringes with needles built in the machine, and an image analysis software (see Fig. 2). During the measurement, a live picture of the probe liquid drop on the sample surface was captured with the CCD camera and the software determined the contact angle between liquid and asphalt. The measurement was performed at room temperature (i.e. about 22°C). Each liquid was individually dropped at seven different locations on the asphalt film and the contact angles were measured. The average contact angle was recorded.

Distilled water, glycerol, and formamide were used as test liquids. The surface free energy components for the three probe liquids [15] are listed in Table 2. Each liquid was individually dropped at seven

Table 2. Surface Free Energies for the Test Liquids (22°C).

Test Liquids	γ /($mJ{\cdot}m^{-2}$)	γ^d /($mJ{\cdot}m^{-2}$)	γ^p /($mJ{\cdot}m^{-2}$)
Distilled Water	72.3	18.7	53.6
Glycerol	65.2	28.3	36.9
Formamide	59.0	39.4	19.6

Table 3. Contact Angles between Three Test Liquids and Asphalt Binders before and after Aging.

Asphalt Binder	Aging Procedure		Distilled Water		Glycerol		Formamide	
			Average,°	CV*,%	Average,°	CV,%	Average,°	CV,%
AAD-1	RTFOT	0*min*	105.2	0.27	96.2	0.75	89.1	0.55
		45*mins*	105.6	0.32	100.6	0.48	90.7	0.40
		85*mins*	105.9	0.41	100.5	0.17	89.9	0.42
		130*mins*	105.6	0.75	99.9	0.28	90.7	0.45
		175*mins*	106.6	1.15	100.0	0.19	90.6	0.70
	PAV	RTFO-45	105.8	0.45	99.9	0.25	90.1	0.46
		RTFO-85	106.0	0.48	100.2	0.21	91.0	0.34
		RTFO-130	106.9	0.53	99.5	0.12	91.5	0.27
		RTFO-175	107.5	0.18	100.1	0.64	92.4	0.79
AAK-1	RTFOT	0*min*	103.9	0.49	97.5	0.48	86.7	0.32
		45*mins*	106.0	0.37	97.2	0.52	88.9	0.48
		85*mins*	106.6	0.37	97.5	0.27	88.4	0.32
		130*mins*	107.4	0.22	97.3	0.39	88.8	0.50
		175*mins*	107.1	0.34	97.5	0.03	89.5	0.55
	PAV	RTFO-45	105.2	0.11	97.8	0.35	86.9	0.39
		RTFO-85	105.6	0.31	96.5	0.34	87.8	0.19
		RTFO-130	107.3	0.35	97.2	0.32	91.4	0.31
		RTFO-175	107.3	0.37	97.7	0.41	91.4	0.13
AAM-1	RTFOT	0*min*	98.6	0.45	90.7	1.26	76.6	1.02
		45*mins*	96.8	0.53	88.9	0.33	72.9	0.34
		85*mins*	97.8	0.27	89.1	0.48	73.3	0.63
		130*mins*	97.1	0.57	88.7	0.26	73.0	0.36
		175*mins*	96.6	0.39	88.5	0.20	73.2	0.34
	PAV	RTFO-45	96.6	0.55	87.2	0.32	73.2	0.18
		RTFO-85	96.4	0.63	87.3	0.37	73.3	0.29
		RTFO-130	97.3	0.44	87.2	0.34	73.9	0.40
		RTFO-175	96.8	0.34	88.1	0.94	74.7	0.50
AAG-2	RTFOT	0*min*	98.8	1.11	85.7	0.59	75.8	0.69
		45*mins*	94.1	0.42	87.2	0.82	71.5	0.35
		85*mins*	94.3	0.44	86.7	0.37	71.4	0.89
		130*mins*	94.6	0.28	87.0	0.31	71.4	0.25
		175*mins*	94.4	0.32	87.4	0.27	71.3	0.43
	PAV	RTFO-45	94.4	0.28	86.9	0.21	71.4	0.16
		RTFO-85	94.4	0.31	86.8	0.56	71.6	0.30
		RTFO-130	95.3	0.20	87.1	0.18	71.7	0.22
		RTFO-175	94.3	0.23	86.9	0.24	71.6	0.43
ABM-1	RTFOT	0*min*	98.6	0.45	90.7	1.26	76.6	1.02
		45*mins*	94.7	0.37	87.3	0.36	71.2	0.34
		85*mins*	94.9	0.37	87.4	0.19	71.4	0.34
		130*mins*	94.6	0.49	86.5	0.35	72.1	0.86
		175*mins*	94.4	0.50	86.7	0.37	72.0	0.29
	PAV	RTFO-45	95.0	0.28	85.5	0.30	73.2	0.19
		RTFO-85	94.8	0.41	85.3	0.32	73.2	0.21
		RTFO-130	95.2	0.27	85.4	0.42	73.7	0.32
		RTFO-175	95.4	0.42	85.8	0.49	73.8	0.29

*CV-coefficient of variation

different locations on the asphalt film and the contact angles were measured. The average contact angle was recorded as the final result.

Sample Preparation

The asphalt film was made according the following steps. Aluminum plates 15.5*cm* long by 7.5*cm* wide were used as the substrates. The binder was heated at 163°C to flow and then a small amount of asphalt was poured on an aluminum substrate, which had been previously placed on a heater to attain a constant temperature

Fig. 3. Photo of "Doctor-blade".

of 60°C. Then, the asphalt film was created on the aluminum plate using a doctor-blade (Paul N. Gardner Company, USA, see Fig. 3)with a draw-down technique. The asphalt films were cooled down to room temperature and kept in a desiccator overnight before the next step.

Results and Discussion

Influence of Aging on Contact Angle

Table 3 lists the contact angle results between asphalt samples and three test liquids. The coefficients of variation of the contact angles are shown as well. The coefficient of variation equals the standard deviation divided by the mean value. It can be expressed either as a fraction or a percent, which is a useful statistic for comparing the degree of variation from one data series to another, even if the means are drastically different from each other. If the data points are close to the mean, then the coefficient of variation is small. It is found in Table 3 that the coefficients of variations for all the contact angles range from 0.11 to 1.26%, which indicates the test method is repeatable.

The reliability and validity of the contact angle results was assessed with a method developed by Kwok and Neumann [16]. They concluded that the values of $\gamma_1 \cos\theta$ versus γ_1 for a given solid with various liquids should show a linear relationship. If the linearity of the resulting curve is not appropriate, the results need to be remeasured. It was observed that each asphalt sample has a good linear fit between $\gamma_1 \cos\theta$ and γ_1, and the coefficient of determination (R^2) values varies from 0.9557 to 0.9999, as shown in Table 4. This indicates that the contact angle results meet the Kwok's criteria. An illustration of $\gamma_1 \cos\theta$ versus γ_1 for asphalt binder AAD-1 is given in Fig. 4.

It can be seen from the data in Table 3 that the change of each contact angle was not consistent after the asphalt samples were aged by RTFOT/PAV. The contact angles between the three test liquids (distilled water, glycerol, and formamide) and asphalt samples, which were RTFOT aged for different durations and have undergone RTFOT/PAV processes, do not show any obvious regularity. The change trends are fluctuated variations and only a few are increasing/decreasing monotonically, such as the contact angles between glycerol and RTFOT aged AAD-1 samples. It is also noticed that the influences of aging on the contact angles are different as well. For example, after RTFOT aged, for the AAG-2 sample the maximum changes of the contact angles are 0.5° (distilled water), 0.7° (glycerol), and 0.2° (formamide), respectively. However, for AAK-1 sample, the maximum changes of the contact angles are 1.4° (distilled water), 0.3° (glycerol), and 1.1° (formamide), respectively, after RTFOT aged.

If the original binder, RTFOT aged binder, and the corresponding PAV aged binder are considered only, it is found that there exists some regularities. For AAD-1 and AAK-1 samples, the contact angles between the test liquids and the samples increased, except AAK-1-R-85/PAV. For AAM-1 and ABM-1 samples, the contact angles between the test liquids and the samples decreased, except ABM-1-R-45. However, there is no such strong regularity for AAG-2 samples. Wasiuddin et al. [9] also observed that the contact angles between distilled water, formamide and one asphalt binder (PG 64-22) with two types of anti-strip additives increased after RTFOT and PAV process. In contrast, the other sample with PG 70-28 experienced the same procedure, i.e. adding the same two anti-strip additives and RTOT/PAV aging, the contact angles between distilled water, formamide, and the samples reduced. This phenomenon is similar to the results in this study, which means the influence of aging on the contact angle is a kind of complex.

It is known that the wettability of a liquid on a solid can be characterized by the value of the contact angle between them. Generally, the greater the contact angle is, the worse the wetting ability of this liquid on this solid. If the contact angle is 0°, it is called fully wetting or spreading; if the contact angle is less than 90°, it is called partial wetting; if the contact angle is more than 90°, it is named non-wetting [17]. Because the moisture damage is one of the main failures of the asphalt pavement, the changing in contact angles between the distilled water and the asphalt samples will be discussed specially. Based on previous analysis, it is known that after the original binders were subjected to RTFOT (45, 85, 130, and 175*mins*) and PAV aging, the contact angles between distilled water and AAD-1, AAK-1asphalt samples increased. For AAM-1 and ABM-1 samples, the contact angles reduced after RTFOT and PAV aging (except ABM-1-R-45). Although there is no apparent regularity of changing in the contact angles between the three test liquids and AAG-2 samples, it is found that the contact angles between distilled water and AAG-2 samples have the trend of decreasing after RTFOT and PAV aging. Asphalt binder is a kind of hydrophobic material, and the contact angles between distilled water and asphalt samples are all higher than 90° according the data in Table 3, which means asphalt cannot be wetted. However, through the above description, it still can be concluded that after aging the hydrophobicity of the AAD-1 and AAK-1 samples were increased, while the hydrophobicity of the AAM-1, AAG-2, and ABM-1 samples were reduced.

Influence of Aging on Surface Free Energy

The surface free energy and its components (polar and dispersion part) of the asphalt samples are given in Table 5. According to Eq. (4), all coefficients of determination between $\frac{(1+\cos\theta)}{2}\frac{\gamma_1}{\sqrt{\gamma_1^{\mathrm{d}}}}$ and $\sqrt{\frac{\gamma_1^{\mathrm{p}}}{\gamma_1^{\mathrm{d}}}}$ of asphalt samples are listed in Table 6, which range between 0.8918 through 0.9999. The coefficient of determination for asphalt AAD-1 is graphically illustrated in Fig. 5.

Table 4. Coefficient of Determination (R^2) between $\gamma_1 \cos\theta$ and γ_1.

Asphalt Binder	Aging Procedure		Coefficient of Determination (R^2)
AAD-1	RTFOT	0*min*	0.9999
		45*mins*	0.9739
		85*mins*	0.9777
		130*mins*	0.9886
		175*mins*	0.9934
	PAV	RTFO-45	0.9868
		RTFO-85	0.9894
		RTFO-130	0.9999
		RTFO-175	0.9999
AAK-1	RTFOT	0*min*	0.9835
		45*mins*	0.9993
		85*mins*	0.9998
		130*mins*	0.9971
		175*mins*	0.9966
	PAV	RTFO-45	0.9920
		RTFO-85	0.9993
		RTFO-130	0.9782
		RTFO-175	0.9865
AAM-1	RTFOT	0*min*	0.9798
		45*mins*	0.9695
		85*mins*	0.9781
		130*mins*	0.9749
		175*mins*	0.9748
	PAV	RTFO-45	0.9912
		RTFO-85	0.9896
		RTFO-130	0.9970
		RTFO-175	0.9887
AAG-2	RTFOT	0*min*	0.9780
		45*mins*	0.9557
		85*mins*	0.9669
		130*mins*	0.9666
		175*mins*	0.9571
	PAV	RTFO-45	0.9660
		RTFO-85	0.9682
		RTFO-130	0.9753
		RTFO-175	0.9656
ABM-1	RTFOT	0*min*	0.9996
		45*mins*	0.9617
		85*mins*	0.9629
		130*mins*	0.9803
		175*mins*	0.9733
	PAV	RTFO-45	0.9974
		RTFO-85	0.9976
		RTFO-130	0.9993
		RTFO-175	0.9983

As seen from Table 5, there seems to be no apparent relationship between the surface free energy and the RTFOT aging time and RTFOT/PAV aging. The surface free energy data have the fluctuated variation. If we only consider the original binder, RTFOT aged binder, and the corresponding RTFOT/PAV aged binder, it looks like some regularities exist. In general, after RTFOT and PAV aging, the surface energies of AAD-1 and ABM-1 samples were reduced, while for AAM-1 samples, the surface energy was increased. For AAK-1 samples, the surface energies decreased except for the following four samples: AAK-1-R-45, AAK-1-R-85, AAK-1-R-85/PAV, and AAK-1-R-130. It should be pointed out that even the surface energy of AAK-1-R-130 increased, the surface energy of its corresponding PAV aged sample decreased to be less than that of the original AAK-1 binder. Hence, this process can be categorized as “decreased surface energy group”.

Table 5. Surface Free Energy and its Components for RTFOT and PAV Aged Asphalt Binders.

Asphalt Binder	Aging Procedure		Surface Free Energy ($mJ \cdot m^{-2}$)		
			Polar	Dispersion	Total
AAD-1	RTFOT	0*min*	1.97	14.54	16.51
		45*mins*	2.29	12.03	14.32
		85*mins*	2.01	12.88	14.88
		130*mins*	2.26	12.25	14.51
		175*mins*	1.83	13.18	15.02
	PAV	RTFO-45	2.05	12.92	14.97
		RTFO-85	2.17	12.29	14.46
		RTFO-130	1.91	12.80	14.71
		RTFO-175	1.84	12.48	14.32
AAK-1	RTFO	0*min*	2.03	14.99	17.02
		45*mins*	1.63	15.15	16.78
		85*mins*	1.34	16.07	17.42
		130*mins*	1.14	16.61	17.75
		175*mins*	1.38	15.53	16.90
	PAV	RTFO-45	1.56	16.03	17.59
		RTFO-85	1.56	16.02	17.58
		RTFO-130	1.66	14.09	15.75
		RTFO-175	1.69	13.84	15.53
AAM-1	RTFOT	0*min*	1.83	22.28	24.11
		45*mins*	2.32	22.55	24.88
		85*mins*	2.25	23.07	25.32
		130*mins*	2.28	22.48	24.77
		175*mins*	2.26	22.86	25.12
	PAV	RTFO-45	1.88	25.11	26.99
		RTFO-85	1.99	24.65	26.64
		RTFO-130	1.73	25.23	26.96
		RTFO-175	2.16	23.19	25.35
ABM-1	RTFOT	0*min*	2.42	22.51	24.93
		45*mins*	2.30	24.81	27.12
		85*mins*	2.26	24.80	27.06
		130*mins*	2.50	24.15	26.64
		175*mins*	2.63	23.75	26.38
	PAV	RTFO-45	2.58	23.73	26.30
		RTFO-85	2.68	23.53	26.21
		RTFO-130	2.58	23.51	26.09
		RTFO-175	2.53	23.44	25.97
AAG-2	RTFOT	0*min*	2.34	24.81	27.15
		45*mins*	2.62	23.83	26.45
		85*mins*	2.53	24.31	26.84
		130*mins*	2.39	24.60	26.99
		175*mins*	2.43	24.37	26.81
	PAV	RTFO-45	2.47	24.39	26.86
		RTFO-85	2.54	24.11	26.65
		RTFO-130	2.11	25.19	27.30
		RTFO-175	2.53	24.13	26.66

Cheng et al. [18],Wasiuddin et al. [9], and Howson et al. [10] had studied the aging effect on surface free energy of asphalt binders. Although the aging processes were different, the main conclusion was similar, which is that aging reduces the surface free energy of asphalt binder. In this study, except for all AAM-1asphalt samples and three AAK-1 asphalt samples, a decrease in surface free energy after aging was observed, which is in line with previous research.

According to Harkins [19], the work of cohesion is two times the surface energy of the asphalt binder. A small work of cohesion indicates that only little work is required to create a unit area crack within the binder or mastic. Walubita et al. [20] also found that the fracture performances of the asphalt binder were deteriorated by

Table 6. Coefficient of Determination between $\frac{(1+\cos\theta)}{2}\frac{\gamma_1}{\sqrt{\gamma_1^d}}$ and $\sqrt{\frac{\gamma_1^p}{\gamma_1^d}}$.

Asphalt Binder	Aging Procedure		Coefficient of Determination (R^2)
AAD-1	RTFOT	0*min*	0.9962
		45*mins*	0.9494
		85*mins*	0.9473
		130*mins*	0.9731
		175*mins*	0.9779
	PAV	RTFO-45	0.9663
		RTFO-85	0.9734
		RTFO-130	0.9976
		RTFO-175	0.9989
AAK-1	RTFOT	0*min*	0.9563
		45*mins*	0.9999
		85*mins*	0.9999
		130*mins*	0.9932
		175*mins*	0.9948
	PAV	RTFO-45	0.9683
		RTFO-85	0.9999
		RTFO-130	0.9669
		RTFO-175	0.9823
AAM-1	RTFOT	0*min*	0.9305
		45*mins*	0.8918
		85*mins*	0.9017
		130*mins*	0.9042
		175*mins*	0.9157
	PAV	RTFO-45	0.9649
		RTFO-85	0.9615
		RTFO-130	0.9843
		RTFO-175	0.9631
AAG-2	RTFOT	0*min*	0.9377
		45*mins*	0.9010
		85*mins*	0.9192
		130*mins*	0.9131
		175*mins*	0.8946
	PAV	RTFO-45	0.9151
		RTFO-85	0.9227
		RTFO-130	0.9232
		RTFO-175	0.9169
ABM-1	RTFOT	0*min*	0.9962
		45*mins*	0.8979
		85*mins*	0.8987
		130*mins*	0.9479
		175*mins*	0.9364
	PAV	RTFO-45	0.9893
		RTFO-85	0.9902
		RTFO-130	0.9953
		RTFO-175	0.9920

long-term aging. In this study, the surface free energy reduced for most asphalt samples after aging, which means the work of cohesion decreased and the binders are easy to crack. This point also verifies Walubita's conclusion [20]. And more laboratory research supplemented with field study is needed to validate this finding. It should be noted that the variation extent of the surface free energy for the studied asphalt binders before and after aging depends on the binder itself, which may be related to the chemical composition and will be studied in the next step.

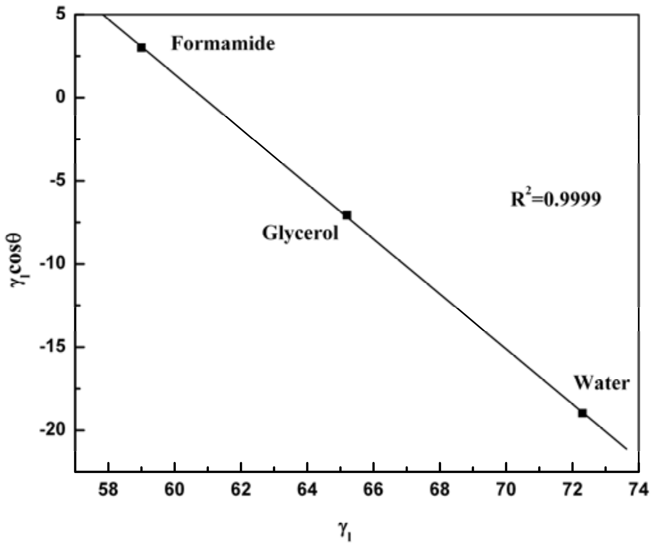

Fig. 4. Illustration of the $\gamma_l \cos\theta$ versus γ_l for AAD-1 Asphalt Binder.

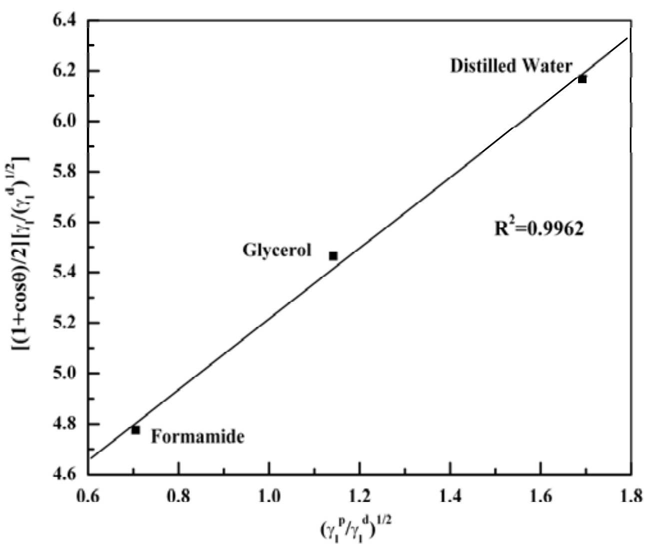

Fig. 5. Use of the Polar and Dispersion Components Asphalt Binder Type AAD-1 to Determine the Regression Coefficient Value.

Conclusions

On the basis of above study, the following conclusions can be drawn.

1. The surface free energy of asphalt binders can be obtained using contact angles between the asphalt binders and different probe liquids, according to the theory developed by Owens and Wendt [14]. And the sessile drop method is a simple way to determine the contact angle between an asphalt binder and various probe liquids, which can be used to calculate the surface free energy.
2. In most cases the surface free energy of asphalt binder was reduced due to RTFO-aging at 163°C for different durations and PAV-aging at 100°C and 2.1*MPa* for 20*hrs*, which indicates that the work of cohesion of asphalt binder is reduced, and consequently the fracture resistance of the binder is decreased as well. The change of surface free energy of asphalt binder due to aging may depend on the chemical composition of the binder.

Nomenclature:

γ — Surface free energy, $mJ{\cdot}m^{-2}$;
θ — Contact angle, °;
γ_l — Surface free energy of liquid, $mJ{\cdot}m^{-2}$;
γ_s — Surface free energy of solid, $mJ{\cdot}m^{-2}$;
γ_{sl} — Interfacial free energy between solid and liquid, $mJ{\cdot}m^{-2}$；
γ_l^d — Dispersion part of surface free energy of liquid, $mJ{\cdot}m^{-2}$;
γ_l^p — Polar part of surface free energy of liquid, $mJ{\cdot}m^{-2}$;
γ_s^d — Dispersion part of surface free energy of solid, $mJ{\cdot}m^{-2}$;
γ_s^p — Polar part of surface free energy of solid, $mJ{\cdot}m^{-2}$.

Superscripts：

d – Dispersion;
p – Polar.

Subscripts：

s – Solid;
l – Liquid;
sl – Interface of solid and liquid.

Acknowledgment

The authors appreciate the Paint and Corrosion Laboratories at Turner-Fairbank Highway Research Center for supplying the DSA 10 equipment to perform the contact angle measurements. The authors gratefully acknowledge the financial assistance provided by the Federal Highway Administration, USA.

References

1. Lu, X. and Isacsson, U., (1998). Chemical and Rheological Evaluation of Ageing Properties of SBS Polymer Modified Bitumens, *Fuel*, 77(9-10), pp. 961-972.
2. Airey, G.D., (2003). State of the Art Report on Ageing Test Methods for Bituminous Pavement Materials, *International Journal of Pavement Engineering*, 4(3), pp. 165-176.
3. Cheng, D.X., (2002). Surface Free Energy of Asphalt-Aggregate System and Performance Analysis of Asphalt Concrete Based on Surface Free Energy, *PhD Dissertation*, College Station, Texas A&M University, Texas, USA.
4. Masad, E., Zollinger, C., Bulut, R., Little, D., and Lytton, R., (2006). Characterization of HMA Moisture Damage Using Surface Energy and Fracture Properties, *Journal of the Association of Asphalt Paving Technologists*, Vol. 75, pp. 713-748.
5. Wasiuddin, N.M., Zaman, M.M., and O'Rear, E.A., (2010). Polymeric Aggregate Treatment Using Styrene-Butadiene

Rubber (SBR) for Moisture-Induced Damage Potential, *International Journal of Pavement Research and Technology*, 3(1), pp. 1-9.

6. Ganghi, T., Xiao, F.P., and Amirkhanian, S.N., (2009). Estimating Indirect Tensile Strength of Mixtures Containing Anti-Stripping Agents Using an Artificial Neural Network Approach, *International Journal of Pavement Research and Technology*, 2(1), pp. 1-12.
7. Hossain, Z., Zaman, M., and Hobson, K.R., (2010). Effects of Liquid Anti-Stripping Additives on Rheological Properties of Performance Grade Binders, *International Journal of Pavement Research and Technology*, 3(4), pp. 160-170.
8. Cheng, D., Little, D.N., Lytton, R.L., and Holste, J.C., (2002). Use of Surface Free Energy Properties of the Asphalt-Aggregate System to Predict Moisture Damage Potential, *Journal of Association of Asphalt Paving Technologists*, Vol. 71, pp. 59-88.
9. Wasiuddin, N.M., Fogle, C.M., Zaman, M.M., and O'Rear, E.A., (2007). Characterization of Thermal Degradation of Liquid Amine Anti-Strip Additives in Asphalt Binders due to RTFO and PAV-Aging, *Journal of Testing and Evaluation*, 35(4), pp. 387-394.
10. Howson, J.E., Bhasin, A., Masad, E., Little, D.N., Lytton, R.L., and Claros, H., (2007). Influence of Material Factors on Surface Free Energy and Performance Related Parameters, *International Conference: Advanced Characterisation of Pavement and Soil Engineering Materials*, pp. 1621-1630, Athens, Greece, CD-ROM.
11. Jones, D.R., (1993). SHRP Materials Reference Library: Asphalt Cements: A Concise Data Compilation, *SHRP-A-645*, pp. 4-27, Washington DC, USA.
12. Young, T., (1805). An Essay on the Cohesion of Fluids, *Philosophical Transactions of the Royal Society of London*, 95, pp. 65-87.
13. Fowkes, F.M., (1964). Dispersion Force Contributions to Surface and Interfacial Tensions, Contact Angles, and Heats of Immersion, *Advances in Chemistry Series*, 43(1), pp. 99-111.
14. Owens, D.K. and Wendt, R.C., (1969). Estimation of the Surface Free Energy of Polymers, *Journal of Applied Polymer Science*, 13(8), pp. 1741-1747.
15. Krüss Company, (2002), *Drop Shape Analysis Software: Liquid Database*, Krüss Company, Germany.
16. Kwok, D.Y. and Neumann, A.W., (1999). Contact Angle Measurement and Contact Angle Interpretation, *Advances in Colloid and Interface Science*, 81(3), pp. 167-249.
17. Hiemenz, P.C. and Rajagopalan, R., (1997). *Principles of Colloid and Surface Chemistry*, Third Edition, Marcel Dekker, Inc., New York, USA.
18. Cheng, D., Little, D.N., Lytton, R.L., and Holste, J.C., (2002). Surface Energy Measurement of Asphalt and Its Application to Predicting Fatigue and Healing in Asphalt Mixtures, *Transportation Research Record*, No. 1810, pp. 44-53.
19. Harkins, W.D., (1952). *The Physical Chemistry of Surface Films*, pp. 199-210, Reinhold, New York.
20. Walubita, L.F., Martin, A.E., Glover, C., Jung, S.H., Cleveland, G., and Lytton, R.L., (2005). Fatigue Characterization of HMAC Mixtures Using Mechanistic Empirical and Calibrated Mechanistic Approaches Including the Effects of Aging, *Geotechnical Special Publication: Asphalt Concrete: Simulation, Modeling, and Experimental Characterization (GSP 146)*, ASCE, pp. 103-114.